Optimizing bioconversion pathways through systems analysis and metabolic engineering

Daniel E. Stafford*, Kurt S. Yanagimachi*, Philip A. Lessard†, Sushil K. Rijhwani*, Anthony J. Sinskey†, and Gregory Stephanopoulos*‡

Departments of *Chemical Engineering and †Biology, Massachusetts Institute of Technology, Cambridge, MA 02139

Communicated by Boris Magasanik, Massachusetts Institute of Technology, Cambridge, MA, December 18, 2001 (received for review October 18, 2001)

We demonstrate a general approach for metabolic engineering of biocatalytic systems comprising the uses of a chemostat for strain improvement and radioisotopic tracers for the quantification of pathway fluxes. Flux determination allows the identification of target pathways for modification as validated by subsequent overexpression of the corresponding gene. We demonstrate this method in the indene bioconversion network of *Rhodococcus* modified for the overproduction of 1,2-indandiol, a key precursor for the AIDS drug Crixivan.

Complex metabolic and bioconversion pathways containing parallel, branching, and/or reversible reactions can be studied quantitatively under the framework of metabolic engineering, which uses steady-state fluxes as fundamental determinants of cell physiology (1, 2). It is necessary to use these methods to distinguish the relative importance of competing metabolic reactions to guide target selection for the improvement of biological production of secondary metabolites or small molecules important for pharmaceutical and materials applications (3). To date, applications of metabolic engineering have been limited to primarily linear pathways and cases in which the relevant biochemistry and associated genetics are well established. In many cases, efforts focusing on transformation of cells by ad hoc methods have failed where genes are introduced based on conclusions derived in the absence of quantitative analysis of pathways. Consequently, an approach that considers the systemic properties of a bioconversion to identify rational targets is valuable. Such an approach can be based on determination of fluxes in bioconversion networks, which has been a focus of metabolic engineering for the past 10 years.

We have developed and applied a general framework for the optimization of bioconversion systems in the context of the directed biocatalytic production of *trans*-(1*R*,2*R*)-indandiol suitable for the synthesis of the HIV protease inhibitor Crixivan (Merck). Chartrain *et al.* (4) isolated *Rhodococcus* sp. I24, which possesses the required oxygenase enzyme activities for converting indene to (2*R*)-indandiol (Fig. 1). The Crixivan chiral precursor (−),-*cis*-(1*S*,2*R*)-1-aminoindan-2-ol [(−)-CAI] can then be synthesized from (2*R*)-indandiol through a Ritter reaction (5, 6). However, besides the desired (2*R*)-indandiol product, several other side-products are secreted also in a *Rhodococcus* sp. I24 fermentation that reduce the desired product yield and selectivity. Therefore, it is of interest to modify I24 genetically to eliminate undesirable reactions and enhance the product-forming pathway. Because of the poorly characterized nature of I24 genetics *a priori*, it is imperative that an approach be developed to prioritize network targets for modification in light of the current state of knowledge of the given biological system.

The general framework described here is comprised of five essential steps: (*i*) establishment of an experimental system for strain selection and metabolic network analysis, (*ii*) definition of the bioconversion network, (*iii*) quantification of network fluxes, (*iv*) target identification, and (*v*) flux redistribution. In this study, a systematic evaluation of the physiology of *Rhodococcus* strains and determination of the relative fluxes of the indene bioconversion network facilitated the improvement of (2*R*)-indandiol production suitable for Crixivan manufacturing.

Materials and Methods

Bacterial Growth and Preparation of Cell Lysates. *Rhodococcus* sp. I24 was isolated by Merck scientists from soil contaminated with toluene (7). Strain KY1 was isolated during a continuous fermentation of I24. Stock culture vials of I24 and KY1 were stored at −80°C in LB medium supplemented with 25% glycerol. Working cultures of all strains were grown and maintained on LB plates streaked from frozen stocks. KY1 cultures were cultivated at 30°C in LB medium, whereas KY1(pDS3) and KY1(pAL282) cultures required 10 μg/ml gentimicin sulfate for selection.

Cell lysates were prepared by centrifuging the cells at 14,000 × *g*. The supernatant was removed, and the cells were washed in lysis buffer containing 100 mM Hepes, 10% glycerol, 0.2 mM β-mercaptoethanol, and 2 tablets per 50 ml of protease inhibitor mixture (Complete, EDTA-free, Roche Molecular Biochemicals) at pH 7.0 and 4°C. The cells were centrifuged and resuspended in lysis buffer at 4°C. The cells were passed through a prechilled French press at 16,000 psi three times. The crude lysate was cleared by centrifugation, and the top fraction was collected and stored at −20°C until use.

Reagents. [^{14}C]indene [425 μCi/ml (1 Ci = 37 GBq) in aqueous ethanol solution] and (1*S*,2*R*)-indan oxide [84% enantiomeric excess (ee), 93% purity, 1,075 mg/ml ethanol] were supplied by Merck Research Laboratories, Rahway, NJ. Fine chemicals were purchased from Sigma Aldrich except where noted. Restriction enzymes and DNA-modifying enzymes were purchased from New England Biolabs and used according to the manufacturer's recommendations. PCR was carried out by using the PCR Core kit (Roche, Indianapolis, IN). Primers for PCR were purchased from GIBCO/BRL.

Fermentation System. A VirTis Omni-Culture base was used with a 2.0-liter capacity vessel (New Brunswick Scientific) and custom-made head plate. The base controlled the fermentation temperature at 30 ± 1°C and agitation speed at 1,000 ± 5 rpm. The pH was maintained at 7.0 ± 0.1 by the addition of filtered 2 M NaOH. For high-pH fermentations, Tris base was added to a final concentration of 20 mM after initiation of indene metabolite production. Filter-sterilized air feed was maintained at 1.0 liter/min with Cole-Parmer gas mass-flow controllers.

Media. Initial I24 cultures were grown in complex medium as described by Chartrain *et al.* (4) for the 23-liter scale fermentations except the 20 g/liter glycerol was substituted with glucose (Fisher), and the Mops (Sigma) was decreased to 1.0 g/liter.

Abbreviation: ee, enantiomeric excess.

‡To whom reprint requests should be addressed at: Massachusetts Institute of Technology, Room 56-469C, Cambridge, MA 02139. E-mail: gregstep@mit.edu.

The publication costs of this article were defrayed in part by page charge payment. This article must therefore be hereby marked "*advertisement*" in accordance with 18 U.S.C. §1734 solely to indicate this fact.

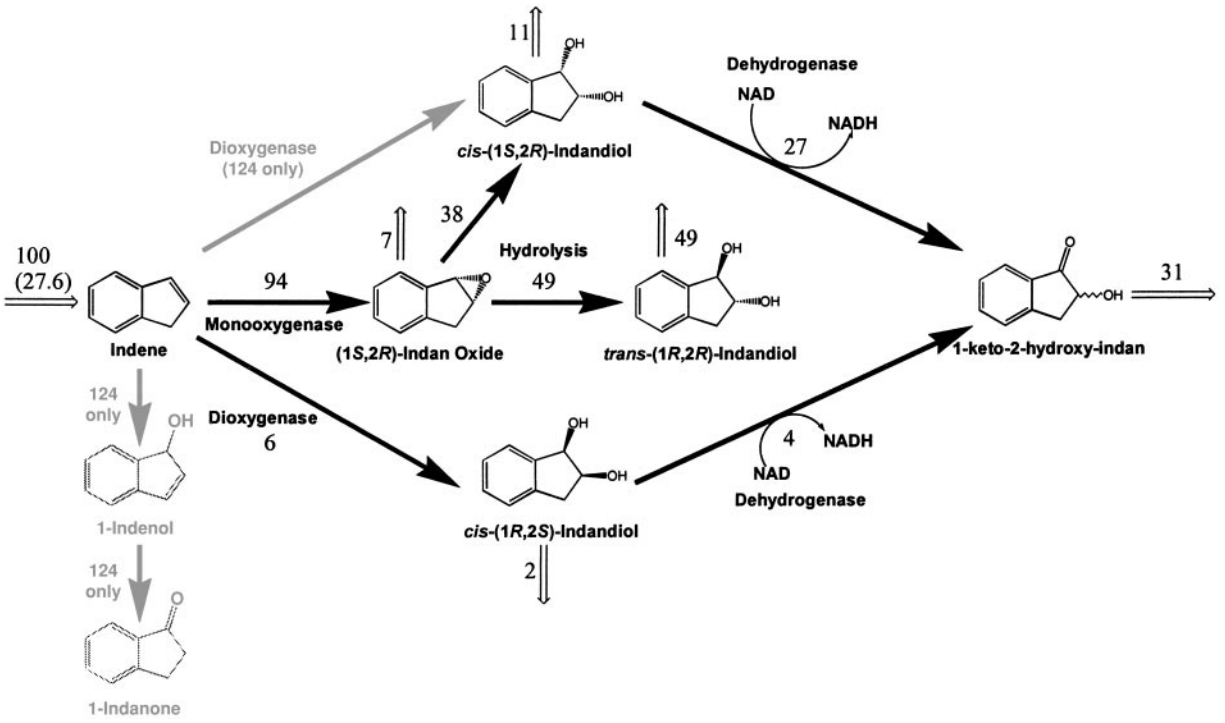

Fig. 1. Indene bioconversion network in *Rhodococcus* sps. I24 and KY1 and steady-state flux distribution for KY1 at 100 ppm indene air-feed concentration and a dilution rate of 0.065 h^{-1}. The oxygenation reactions shaded in gray are observed in I24 only. The fluxes were normalized by the indene uptake rate (in parentheses, μmol·h^{-1} per g of dry cell weight). The solid arrows denote intracellular fluxes, and open arrows indicate indene uptake and metabolite excretion fluxes.

Subsequent I24 and KY1 cultures were grown in defined media optimized for maximum biomass accumulation in shake flasks (unpublished work). The defined fermentation medium contained 40 g/liter glucose, 1.4 g/liter $(NH_4)_2SO_4$, 1.0 g/liter $MgSO_4 \cdot 7H_2O$, 0.015 g/liter $CaCl_2 \cdot 2H_2O$, 1.0 g/liter Mops buffer, 1.0 ml/liter A9 trace elements solution, 1.0 ml/liter Stock A solution, 35.2 ml/liter 1.0 M phosphate buffer, and 1.0 ml/liter polypropylene glycol (molecular weight, 2,000). The stock solutions were the same as those used by Chartrain *et al.* (4) for their isolation of toluene- and xylene-degrading microorganisms.

Bioconversions. The fermentor was inoculated with 25 ml of preculture grown in a shake flask. Both the medium and indene feeds were initiated when the fermentor culture reached an OD_{600} of ≈15, corresponding to midexponential growth of the culture. The feed medium was the same as the respective fermentor medium except 25 ml/liter 1 M phosphate buffer was used instead of 35.2 ml/liter in the KY1 chemostat. For continuous cultures, a constant volume of 1 liter was maintained in the fermentor. Indene bioconversions performed in batch mode used the same fermentation system and defined medium except for the addition of 10 mg/liter gentimicin for selection where appropriate. The defined medium described above was used for cell growth, because indene is not used as a carbon source by the strains described here. The indene feed was initiated when the fermentor culture reached an OD_{600} of ≈5 (early exponential growth).

The indene and other inducers (naphthalene and toluene) were fed separately to the fermentor by using an air-delivery system consisting of two air streams: one air stream was passed through the appropriate inducer contained in a flask and then combined with another air stream to dilute the inducer air concentration. The flow rates of each air stream were adjusted for a total flow rate of 1.0 liter/min with the desired inducer concentration. The inducer concentration was measured by using a Pine Environmental Services Photovac 2020 photoionization detector set with a response factor of 0.3 for both indene and naphthalene and 0.5 for toluene.

^{14}C-Tracer Experiments. A 15-ml culture sample was removed from the chemostat under steady-state conditions (constant biomass concentration after at least four residence times) during induction. The sample was placed in a 125-ml screw-cap shake flask. [^{14}C]indene stock (50 μl) was added immediately to the flask. The flask was sealed and placed in a shaker at 300 rpm, 30°C. Samples were taken intermittently for 2 h after the addition of [^{14}C]indene.

HPLC Assays. Indene metabolite concentrations were measured by using a reverse-phase HPLC assay with a Zorbax RX-C8 column (4.6 mm × 25 cm, Hewlett–Packard) and a separate chiral assay using a normal phase HPLC Chiralpak AD column (Chiral Technologies, Exton, PA) as described by Chartrain *et al.* (4). ^{14}C radioactive counts were measured as described elsewhere (8). The ee of the *cis*-[^{14}C]indandiol in the ^{14}C-tracer studies was calculated by using the total counts of each enantiomer separated by using an HPLC assay with a Chiralpak OJ column running an isocratic elution of 90% hexane and 10% isopropyl alcohol as described elsewhere (9).

Plasmid Construction. The *limA* gene (GenBank accession no. Y18005) was synthesized artificially based on the published sequence and then inserted downstream of a truncated λ P_L promoter in a Gent^R plasmid, pDS3, capable of replication in both *Escherichia coli* and *Rhodococcus* sp. KY1 (Fig. 2; ref. 10). The blank control plasmid pAL282 was prepared by deleting the *Eco*RI restriction fragment that contained the *limA* ORF from pDS3.

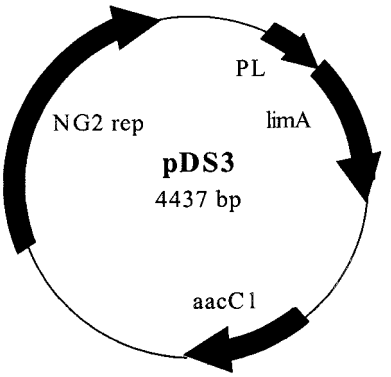

Fig. 2. Diagram of pDS3, which expresses the *limA*-encoded epoxide hydrolase in *Rhodococcus* sp. KY1 from the constitutive λ P_L promoter. *aacC1*, gentamicin resistance marker from Tn1696; NG2 rep, origin of replication derived from pEP2.

Epoxide Hydrolase Activity Assay. Cell lysate (1–5 ml) was placed in a 125-ml screw-cap shake flask, and (1*S*,2*R*)-indan oxide (83% ee) was added to a final concentration of 8 mM. The lysate was incubated at 30°C and agitated at 300 rpm. HPLC analysis was performed as described above.

Indan Oxide Hydrolysis Assay. Culture medium (10 ml), adjusted from pH 5.0–10.0, was placed in a 125-ml screw-cap shake flask, and (1*S*,2*R*)-indan oxide (83% ee) was added to a final concentration of 1.0 mM. The flasks were incubated at 30°C and agitated at 300 rpm. Samples were taken for HPLC analysis for 12 h after indan oxide addition.

Results

Experimental System for Strain Improvement and Network Analysis. A gas-phase indene-delivery system was developed and implemented in chemostat operation for indene bioconversion. Physiological studies using metabolic flux analysis are carried out preferably in continuous flow systems that can attain a metabolic steady state. Steady states were obtained at different indene air-feed concentrations below 200 ppm and dilution rates below 0.10 h^{-1}. Indene-feed concentrations above 200 ppm were toxic to the cells in the chemostat, resulting in cell washout. I24 was grown in the chemostat at a dilution rate of 0.10 h^{-1} under indene air-feed concentrations of 85 and 120 ppm.

At the initial steady state of 85 ppm indene air feed concentration, *cis*-indandiol, 1-indenol, 1-indanone, and 1-keto-2-hydroxy-indan were observed (Fig. 3). The first three products are hypothesized to be caused by a toluene-inducible dioxygenase activity in I24 similar to that observed in *Pseudomonas* (11). A new steady state was sought by increasing the indene-feed concentration to 120 ppm. After ≈200 h of continuous operation, distinct changes in the indene metabolite concentration profiles were evident. 1-indenol and 1-indanone were no longer produced by the cells and were washed out of the chemostat. Concurrent with this change, indan oxide and *trans*-indandiol production was detected, whereas the *cis*-indandiol concentration decreased and the 1-keto-2-hydroxy-indan concentration increased from their previous steady-state levels. These changes suggest that a mutant strain deficient in the oxygenase activity producing 1-indenol and 1-indanone was selected in the chemostat. A second chemostat running in parallel under similar conditions exhibited very similar behavior. Furthermore, cells obtained at the end of these runs were isolated and found to be stable in terms of the excreted array of metabolites for over 900 h in subsequent chemostat runs. The (2*R*)-indandiol yield and selectivity for KY1 increased up to 2-fold relative to I24 (Table 1). The appearance of KY1 suggests that the genes encoding the oxygenase enzyme(s) responsible for 1-indenol and 1-indanone biosynthesis were mutated. A Southern hybridization analysis of I24 and KY1 genomic DNA revealed that there were significant deletions in the KY1 genome, mostly in a 340-kb megaplasmid that resides in I24 but was not detected in KY1 (unpublished data).

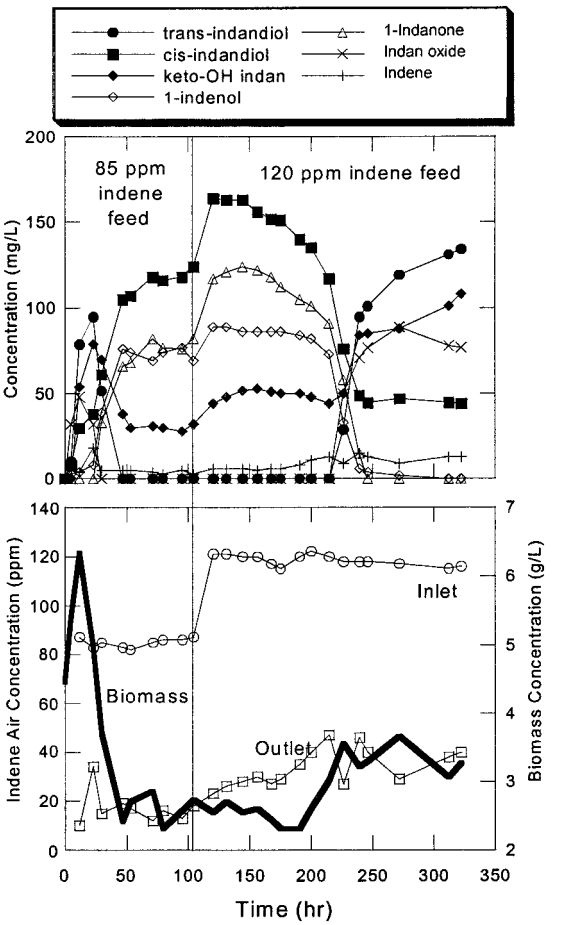

Fig. 3. Transients for States A (0.10 h^{-1} dilution rate and 85 ppm indene air feed) and B (0.10 h^{-1} dilution rate and 120 ppm indene air feed) in the *Rhodococcus* sp. I24 chemostat. Behavior characteristic of KY1 is exhibited after 250 h.

The emergence of the KY1 strain validates the role of a chemostat in metabolic engineering as a selective tool for strain improvement, particularly for cases in which elimination of reactions giving toxic side-products is desired. The isolation of KY1 highlights the rather unconventional use of the chemostat for the evolution of strains with improved bioconversion properties, which contrasts with its traditional application to cell-physiology studies. In this unique case, the bioconversion substrate (indene) is decoupled from the growth substrate (glucose), and cell growth presumably is limited by the toxic nature of indene and not the absence of a critical substrate. This unusual feature of indene bioconversion allowed us to maintain the biocatalyst under well defined environmental conditions with respect to both substrates for the purpose of strain selection and to simultaneously study the effect of the bioconversion substrate on cell physiology through the quantification of network fluxes. In this sense, the chemostat allowed us to (*i*) define a steady environment and apply selective pressure to I24, which resulted in the isolation of KY1, and (*ii*) systematically study the different steps of the bioconversion process. The details of this second

Table 1. Steady-state concentrations and specific productivities of *Rhodococcus* chemostat cultures

	Strain 124		Strain KY1			
	D = 0.10 h^{-1}		D = 0.10 h^{-1}		D = 0.065 h^{-1}	
Steady-state values	85 ppm	120 ppm	100 ppm	170 ppm*	100 ppm	170 ppm
trans-(1*R*,2*R*)-indandiol, mg/liter	0	0	86	181	151	262
cis-(1*R*,2*S*)-indandiol, mg/liter	18	23	6	8	5	8
cis-(1*S*,2*R*)-indandiol, mg/liter	106	129	24	52	35	55
1-Keto-2-hydroxy indan, mg/liter	32	51	25	93	96	154
1-Indenol, mg/liter	69	86	0	0	0	0
1-Indanone, mg/liter	82	118	0	0	0	0
Indan oxide, mg/liter	0	0	21	42	34	55
Indene, mg/liter	3	6	10	14	5	6
Biomass, grams per dry cell weight per liter	2.7	2.4	3.2	3.6	4.9	3.7
(2*R*)-Diol productivity, μmol·h^{-1} per g of dry cell weight	26	36	23	43	18	35
(2*R*)-Diol yield, μmol of diol/μmol of indene	0.32	0.30	0.66	0.61	0.62	0.55
(2*R*)-Diol selectivity†‡	0.32	0.30	0.61	0.54	0.53	0.55
Indene uptake rate (material balance)§	ND	ND	35 ± 5	71 ± 5	29 ± 2	64 ± 5
Indene uptake rate (air measurement)§	ND	ND	40 ± 7	62 ± 12	28 ± 5	63 ± 10

*These values are from a pseudo-steady state during oscillations when the concentrations were constant for one residence time.
†(2*R*)-Diol selectivity for strain I24 is defined as (concentration of *cis*-(1*S*,2*R*)-indandiol)/(concentration of all indene metabolites).
‡(2*R*)-Diol selectivity for strain KY1 is defined as (concentration of *trans*-indandiol)/(concentration of *trans*-indandiol and undesired byproducts), where the undesired byproducts are both *cis*-indandiol enantiomers and 1-keto-2-hydroxy-indan.
§Uptake rates are in μmol·h^{-1} per g of dry cell weight. ND, not determined.

application of the chemostat to indene bioconversion are provided below.

Definition of the Indene Bioconversion Network. To characterize the physiological differences between strains I24 and KY1, the strains were cultivated in separate chemostats and, after steady states were attained, were induced by toluene, naphthalene, or indene. The physiological state of the culture was evaluated by probing the corresponding monooxygenase and dioxygenase activities with the introduction of [^{14}C]indene and measuring the concentrations of the primary oxygenated [^{14}C]indene products. The rate of depletion of this tracer provided a measure of the actual *in vivo* activity of these enzymes because of the rapid uptake of the labeled substrate (8). In I24, toluene induces oxygenase activity converting indene to *cis*-(1*S*,2*R*)-indandiol (35% ee) and 1-indenol as observed previously (4), with the 1-indenol isomerizing to 1-indanone. Conversely, KY1 does not convert the [^{14}C]indene at a significant rate under toluene induction. Only trace amounts of [^{14}C]indan oxide were detected after 2 h, similar to the uninduced profiles of both strains I24 and KY1, attributable to the enzyme induction caused by the tracer itself. Therefore, KY1 seems to either be defective in the mechanism of toluene induction, contain a mutated gene encoding an inactive toluene-inducible dioxygenase, or lack some portion of this dioxygenase gene altogether.

Under naphthalene induction, the ^{14}C product profiles for I24 and KY1 were virtually identical. The [^{14}C]indene was converted completely to *cis*-indandiol and 1-indenol within 5 min. The only subtle difference between the two strains was that I24 produces *cis*-(1*R*,2*S*)-indandiol of 77% ee, whereas KY1 produces *cis*-(1*R*,2*S*)-indandiol of >99% ee. The *cis*-(1*R*,2*S*)-indandiol and 1-indenol are believed to be products of a naphthalene-inducible dioxygenase (NidAB) characterized previously (12). The enantiomeric mixture of *cis*-indandiol produced by I24 (also observed by Chartrain, *et al* in ref. 4) indicates that cross-induction is occurring between at least two dioxygenases in I24. This cross-induction does not occur in KY1 because of its altered or deleted toluene-inducible dioxygenase gene.

As expected, strains I24 and KY1 exhibited drastically different ^{14}C-transient metabolite profiles under indene induction. In I24, *cis*-(1*S*,2*R*)-indandiol (32% ee) and 1-indenol were the primary products formed. KY1 did not exhibit this toluene-induced dioxygenase activity and instead produced indan oxide through a proposed monooxygenase enzyme. Furthermore, it was found that in a cell-free environment, indan oxide hydrolyzes, forming only (2*R*)-indandiols (8), suggesting that only the (1*S*,2*R*)-indan-oxide enantiomer is synthesized by the monooxygenase activity. Indan oxide hydrolysis is not catalyzed by an endogenous epoxide hydrolase activity as confirmed with (1*S*,2*R*)-[^{14}C]indan oxide tracer experiments with both whole cells and cell lysates. Under standard culture conditions (pH 7.0), the *trans*-(1*R*,2*R*)-indandiol and *cis*-(1*S*,2*R*)-indandiol accumulate at a 4:3 ratio. Additionally, KY1 lacks a significant dehydrogenase activity converting *trans*-(1*R*,2*R*)-indandiol to 1-keto-2-hydroxy-indan (8).

^{14}C-tracer results, together with evidence showing genetic deletions in KY1, indicate that KY1 lacks a toluene-induced dioxygenase activity responsible for the conversion of indene to *cis*-(1*S*,2*R*)-indandiol and 1-indenol. The *cis*-(1*S*,2*R*)-indandiol formed by KY1 results from nonenzymatic hydrolysis of (1*S*,2*R*)-indan oxide produced from indene-induced monooxygenase activity. Under indene-induced conditions, the naphthalene dioxygenase in KY1 is largely inactive, as suggested by the lack of 1-indenol or 1-indanone produced. The pathway for indene bioconversion in KY1 based on this evidence was modified as shown in Fig. 1.

Quantification of Network Fluxes. Because of its branched nature, the KY1 indene bioconversion network constitutes an *underdetermined* system requiring, as such, additional constraints for complete determination and confirmation of the pathway fluxes depicted in Fig. 1 for a representative steady state (0.065 h^{-1} dilution rate and 100 ppm indene air feed concentration; ref. 8). Additional information was generated by ^{14}C-tracer experiments in the form of (*i*) measures of the flux split ratio to *trans*- and *cis*-(2*R*)-indandiol formation from indan oxide hydrolysis, (*ii*) redundant measurement of the indene uptake flux determined from the chemostat gas-phase measurements, and (*iii*) direct calculation of the *trans*-(1*R*,2*R*)-indandiol dehydrogenase flux (8). These fluxes were determined by solving the metabolite

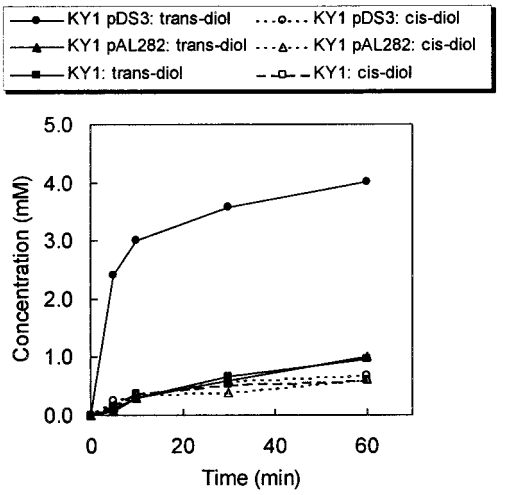

Fig. 4. Conversion of 8.0 mM (1*S*,2*R*)-indan oxide (83% e.e.) to *trans*-indandiol and *cis*-indandiol by lysates prepared from *Rhodococcus* sp. KY1 transformants. Accumulation of *cis*-indandiol in all strains and *trans*-indandiol in KY1 and KY1(pAL282) was equivalent within ± 0.1 mM experimental error.

balances for the system of reactions depicted in Fig. 1 using metabolite uptake and excretion rates determined from steady-state metabolite data (Table 1) with the additional constraints generated by the ^{14}C-tracer experiments described above. It is noted that under all conditions investigated, the flux through the monooxygenase enzyme accounted for at least 94% of the total indene converted.

Target Identification. The results of this flux analysis and the state of knowledge regarding *Rhodococcus* genetics point to the selective hydrolysis of indan oxide to *trans*-(1*R*,2*R*)-indandiol as the key target for improving (2*R*)-indandiol selectivity further. This type of transformation is catalyzed by epoxide hydrolases (13, 14) for many arene oxides including indan oxide (15). This pathway change would favor the formation of the final desirable product, *trans*-(1*R*,2*R*)-indandiol, at the expense of the by-product 1-keto-2-hydroxy-indan. Furthermore, the simplicity of this modification makes it vastly preferable relative to the multiple knockouts of dehydrogenases and/or undesired oxygenases that could alternatively be pursued toward the same objective.

Flux Redistribution. To implement the change suggested from flux analysis, the *limA* gene encoding the *Rhodococcus erythropolis* DCL14 limonene-1,2-epoxide hydrolase (16–18) was constructed by template-free PCR and placed in the expression plasmid pDS3 (Fig. 2). After the addition of (1*S*,2*R*)-indan oxide to KY1(pDS3) cell lysate, a significant increase in the rate of formation of *trans*-indandiol was observed relative to that of KY1 and controls (Fig. 4). SDS/PAGE of the crude lysates showed a clear band at 17 kDa, which is the predicted size of this epoxide hydrolase (17).

We subsequently tested the ability of the recombinant strain KY1(pDS3) to preferentially convert indene to *trans*-indandiol in batch bioconversions. KY1(pDS3) showed an improved overall indene conversion selectivity to *trans*-indandiol over that observed for KY1 batch cultures (Fig. 5 *A* and *B*). As expected, the indene metabolite profiles observed in the control KY1(pAL282) bioconversion were consistent with those obtained with the KY1 parent strain. The improvement exhibited by KY1(pDS3) was pronounced during the initial period of the fermentation. For ≈25 h after the addition of indene, *trans*-indandiol was the primary terminal product formed with an

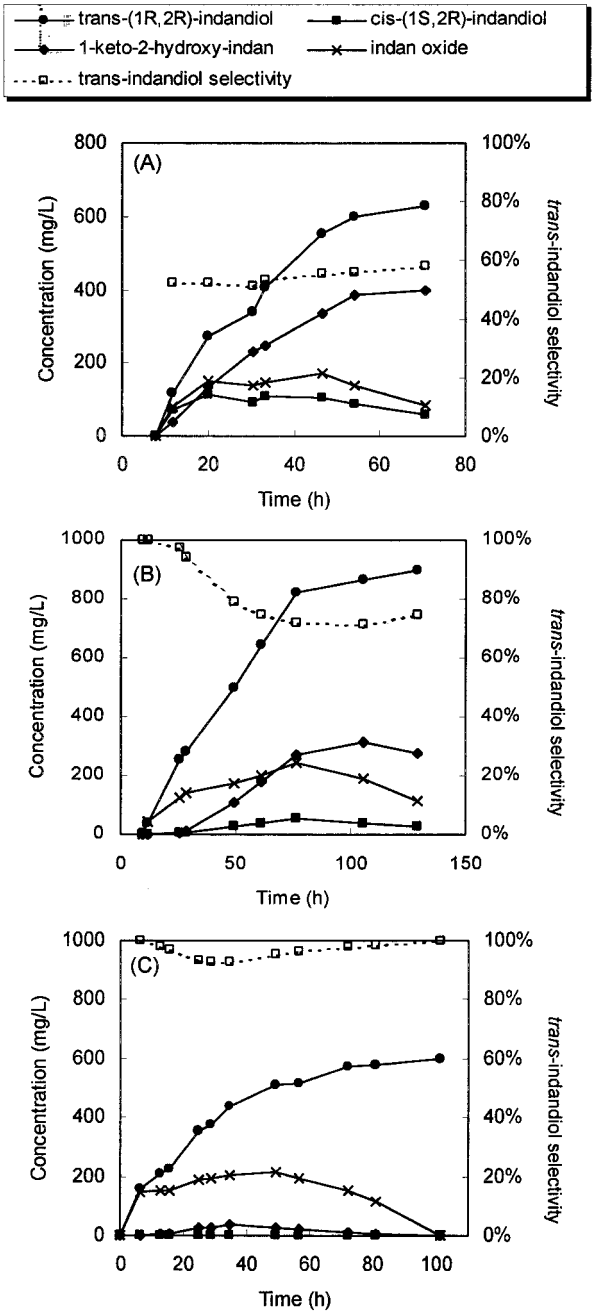

Fig. 5. Indene bioconversion profiles and *trans*-indandiol selectivity in batch cultures of *Rhodococcus* sp. KY1 transformants: *A*, KY1 pAL282 (positive control with blank plasmid), pH 7.0; *B*, KY1(pDS3), pH 7.0; *C*, KY1(pDS3), pH 8.6. Indene was added at 75 ± 10 ppm in 1.0-vvm air. Selectivity is defined as (concentration of *trans*-indandiol)/(concentration of *trans*-indandiol + concentrations of undesired by-products), where the undesired by-products are both *cis*-indandiol enantiomers and 1-keto-2-hydroxy-indan.

average selectivity of ≈95%, which presumably resulted from the newly introduced epoxide hydrolase activity on the (1*S*,2*R*)-indan oxide formed by the indene monooxygenase. After this initial period, indan oxide began to accumulate, and *cis*-(1*S*,2*R*)-indandiol and 1-keto-2-hydroxy-indan accumulated after indan oxide reached a concentration of ≈150 mg/liter. This unusual indene bioconversion profile is likely the result of an initial epoxide-hydrolase activity followed, at later times, with the competing nonenzymatic hydrolysis of indan oxide as the oxide

concentration in the extracellular medium increases. The epoxide hydrolase may deactivate with time or be inhibited by the rising concentrations of some indene metabolites. Another possibility is that indan oxide formed by a membrane-bound monooxygenase is accompanied by significant indan oxide efflux to the medium and subsequent nonenzymatic hydrolysis yielding *cis*-indandiol.

Additional studies demonstrated that the flux split ratio of indan oxide hydrolysis is strongly pH-dependant, with *trans*-indandiol being the primary product formed at pH > 7.0. Of particular interest was the dramatic increase in the relative amount of *trans*-indandiol formed at pH 8.0 and higher. At pH 10.0, 97% of the indan oxide was hydrolyzed to *trans*-(1*R*,2*R*)-indandiol (80% ee). The total indan oxide hydrolysis rate is not affected substantially at pH values between 7.0 and 10.0. At lower pH, a substantial increase in both hydrolysis rate and the relative amount of *cis*-(1*S*,2*R*)-indandiol formed was observed.

Consequently, strain KY1(pDS3) was cultivated in a batch fermentor, and after indene-feed initiation and uptake in late-exponential phase, the culture pH was adjusted to 8.6. This culture showed dramatically improved indene bioconversion profiles over previous cultures of either KY1 or KY1(pDS3) at physiological pH (Fig. 5*C*). No more than 25 mg/liter of the by-product 1-keto-2-hydroxy-indan accumulated at any point in the medium compared with ≈300 mg/liter for the KY1(pDS3) (pH 7.0) fermentation. *Trans*-indandiol was produced by KY1(pDS3) (pH 8.6) at greater than 92% selectivity throughout the culture and was resolved to 100% purity by the end of the bioconversion because of the slow degradation of 1-keto-2-hydroxy-indan.

Discussion

This work has applied the concepts and tools of metabolic engineering in creating an effective combination of a new recombinant *Rhodococcus* strain and fermentation environment capable of complete conversion of indene to *trans*-(1*R*,2*R*)-indandiol product. A mutant strain with a drastically improved chiral indandiol product profile was generated by applying proper selective pressure to chemostat cultures of *Rhodococcus* sp. The isolation of the KY1 strain represents a different and potentially valuable application of the chemostat system whereby cells are sustained on a carbon source but are used for the conversion of a different substrate that is fed to the system. The improvement observed with respect to indene bioconversion most likely is caused by a stereospecific monooxygenase of high activity catalyzing the conversion of indene to indan oxide of (2*R*) chirality and the elimination of a toluene-induced dioxygenase pathway. This modification resulted in doubling the product yield with no significant change in productivity at lower indene concentrations. Further productivity increases are obtained by increasing indene-feed concentration (Table 1) presumably caused by greater induction of the monooxygenase activity.

The approach presented here is applicable also to other bioconversion systems where maximal production of chiral intermediates is sought through bioconversion network optimization (19). This study also demonstrates the importance of rigorously defining the bioconversion network and determining the magnitude of the network fluxes to identify targets for selectivity improvement rationally. Flux distributions were instrumental in identifying targets in the bioconversion network for further genetic work in the KY1 strain to eliminate the remaining side-products. Analysis of the metabolic fate of indan oxide in the KY1 bioconversion network revealed the nonenzymatic hydrolysis of this intermediate to both (2*R*)-indandiol diastereomers. This information permitted us to identify the indan oxide hydrolysis reaction as the prime candidate for modulation with the objective of improving (2*R*)-indandiol selectivity. Through two approaches the (2*R*)-indandiol yield and selectivity was increased to at least 90%, as suggested by the KY1 flux distribution. This work has demonstrated that KY1(pDS3) is a potential production strain capable of producing *trans*-(1*R*,2*R*)-indandiol from indene at high selectivity. Further optimization of bioconversion conditions is likely to improve the product titer obtained in this study. In particular, the use of a two-phase system similar to that used previously should minimize exposure of the cells to the possibly toxic and/or inhibitory indene metabolites (4, 7, 20).

The methods and results of this work have broad implications for the design of metabolic engineering approaches to biocatalyst design in so-called "uncharacterized" biological systems with poorly characterized biochemistry and genetics, particularly with respect to the role of chemostats in strain-improvement programs.

We acknowledge X. O'Brien and A. Dexter for Southern blot analysis of KY1 and I24 genomic DNA and technical assistance from J. Cho, J. Wu, and A. Rodal. We also acknowledge the supply by Merck of the I24 strain, (1*S*,2*R*)-indan oxide, and ^{14}C materials (synthesized by M. Braun). This work was funded by a grant from Merck Research Laboratories and by the Engineering Research Program of BES, Department of Energy Grants DE-FG02-94ER-14487 and DE-FG02-99ER-15015. D.E.S. and K.S.Y. were supported in part by National Institutes of Health Biotechnology Training Grant 2T32 GM08334-10.

1. Bailey, J. E. (1991) *Science* **252,** 1668–1675.
2. Stephanopoulos, G. (1999) *Metab. Eng.* **1,** 1–11.
3. Stafford, D. E., Yanagimachi, K. S. & Stephanopoulos, G. (2001) *Adv. Biochem. Eng. Biotechnol.* **73,** 85–101.
4. Chartrain, M., Jackey, B., Taylor, C., Sandford, V., Gbewonyo, K., Lister, L., DiMichelle, L., Hirsch, C., Heimbuch, B., Maxwell, C., *et al.* (1998) *J. Ferment. Bioeng.* **86,** 550–558.
5. Reider, P. (1997) *Chimia* **51,** 306–308.
6. Senanayake, C., Roberts, F., DiMichele, L., Ryan, K., Liu, J., Fredenburgh, L., Foster, B., Douglas, A., Larsen, R., Verhoeven, T. & Reider, P. (1995) *Tetrahedron Lett.* **36,** 3993–3996.
7. Buckland, B., Drew, S., Connors, N., Chartrain, M., Lee, C., Salmon, P., Gbewonyo, K., Zhou, W., Gailliot, P., Singhvi, R., *et al.* (1999) *Metab. Eng.* **1,** 63–74.
8. Yanagimachi, K. S., Stafford, D. E., Dexter, A. F., Sinskey, A. J., Drew, S. W. & Stephanopoulos, G. (2001) *Eur. J. Biochem.* **268,** 4950–4960.
9. Page, P., Carnell, A. & McKenzie, M. (1998) *Synlett* **7,** 774–776.
10. Sambrook, J., Fritsch, E. F. & Maniatis, T. (1989) in *Molecular Cloning: A Laboratory Manual* (Cold Spring Harbor Lab. Press, Plainview, NY).
11. Wackett, L., Kwart, L. & Gibson, D. (1988) *Biochemistry* **27,** 1360–1367.
12. Treadway, S., Yanagimachi, K., Lankenau, E., Lessard, P., Stephanopoulos, G. & Sinskey, A. (1999) *Appl. Microbiol. Biotechnol.* **51,** 786–793.
13. Weijers, C. & de Bont, J. (1999) *J. Mol. Catal. B* **6,** 199–214.
14. Mischitz, M., Kroutil, W., Wandel, U. & Faber, K. (1995) *Tetrahedron* **6,** 1261–1272.
15. Zhang, J., Reddy, J., Roberge, C., Senanayake, C., Greasham, R. & Chartrain, M. (1995) *J. Ferment. Bioeng.* **80,** 244–246.
16. Barbirato, F., Verdoes, J., de Bont, J. & van der Werf, M. (1998) *FEBS Lett.* **438,** 293–296.
17. van der Werf, M. J., Overkamp, K. M. & de Bont, J. A. M. (1998) *J. Bacteriol.* **180,** 5052–5057.
18. van der Werf, M. J., Swarts, H. J. & de Bont, J. A. M. (1999) *Appl. Environ. Microbiol.* **65,** 2092–2102.
19. Panke, S., Wubbolts, M. G., Schmid, A. & Witholt, B. (2000) *Biotechnol. Bioeng.* **69,** 91–100.
20. Connors, N., Chartrain, M., Reddy, J., Singhvi, R., Patel, Z., Olewinshi, R., Salmon, P., Wilson, J. & Greasham, R. (1997) *J. Ind. Microbiol. Biotechnol.* **18,** 353–359.